

Polarization instability in lasers. II: Influence of the pump polarization on the dynamics

Hassina Zeghlache and Arnaud Boulnois

Laboratoire de Spectroscopie Hertzienne, Université des Sciences et Technologies de Lille 1, 59655 Villeneuve d'Ascq Cedex, France

(Received 8 August 1994)

In a previous paper [Phys. Rev. A **52**, 4229 (1995)] a vectorial model has been derived to describe the dynamics of an optical fiber laser output. In this semiclassical theory, the time-dependent behaviors of the two field polarizations are deduced through the interaction between the light and the active atoms which supposes the presence of a vectorial atomic polarization. This paper is devoted to the analysis of the dynamics presented by such a model using the bifurcation theory. An analytical study investigates the parameter space as far as possible and numerical simulations show the presence of various types of behaviors displayed by the two output field polarizations in the domains where the steady states have lost their stability. The influence of the pump polarization is emphasized. The results are in accordance with the experimental observations.

PACS number(s): 42.55.Wd, 42.65.Vh.

INTRODUCTION

In the preceding paper [1] a vectorial model for the OFL was obtained following some assumptions and simplifications such as isotropic orientation of the induced dipole moments in the active atoms (the Nd^{3+} dopants) [2], different losses of the output-field polarizations, adiabatic elimination of the atomic polarization (related to the level lifetimes), presence of a material grating due to the propagation of two different longitudinal frequencies which is mathematically expressed by a spatial expansion of the material variables, homogeneous broadening, etc. The way to get the model is similar to the one used to treat the bidirectional ring laser [3] and the semiconductor bimode laser [4]: the particular form of the oscillation of two modes along the fiber cavity is integrated following a longitudinal Fourier series whose first order leads to a material "grating" via population inversion (longitudinal hole burning). The interaction of the modes with this grating may induce, under some parametric conditions, constructive interferences which are responsible for the oscillation of the disadvantaged mode (or direction). However, a characteristic of the bidirectional model is the instability of the bimode solution for realistic parametric situations corresponding to class-B lasers: the system oscillates stably in one or the other direction. Regular and irregular pulsations between the two modes alternatively occur depending on the space parameter. In contrast, in the semiconductor case, the bimode solution may oscillate stably but for drastic conditions such as the following:

- (i) Very weak regions of reasonable pump parameters or very large and unrealistic pumpings,
- (ii) Very large detunings due to the diffusion of the charge carriers represented by the enhancement parameter (the so-called Henry parameter) [5] which produces the large gain profile of semiconductor responses, and
- (iii) Very different losses between the two oscillating modes (one of them is strongly disadvantaged).

In the present work we shall give a complementary vectorial model where the two transverse polarizations of the output laser are simultaneously oscillating for reasonable parameter values.

A second interest of this theoretical work on the optical fiber laser (OFL) follows the experimental observations which are related to the competition between the transverse polarizations of the field [6]. This dynamical behavior is supposed due to a population effect as is known from other nonlinear optical systems. Being interested by the description of such behaviors presented by the two field polarizations and also by the influence of the pump polarization, we have derived a model including a vectorial atomic polarization which is a statistical sum of vectorial dipole moments induced during the interaction between the field and the active medium. In this way, we have added a transverse distribution of the moments to the longitudinal complexity of the hole-burning description; this distribution is chosen isotropic and produces a partition of the field-matter nonlinearities between the two transverse polarizations. From the mathematical point of view, this leads to one more "population-inversion" variable which directly measures the relative contribution to the two output transverse polarizations of (1) the relative pump and (2) the nonlinear field-medium interaction.

Finally, this model can provide a general understanding of the average influence of the transverse effects (due to the spatial orientation of both the dipole moments and the pump) on the dynamics presented by the laser.

The paper is organized as follows. We first give the main outlines of the model and its steady states, defining the variables and the parameters. The linear stability of the steady states is explored to a large extent in the second section leading to the conclusions that (1) whatever is the pump, the laser always transfers its stability from a monomode oscillation to a bimode (and bipolarized) oscillation and (2) the detunings and pump-orientation effects derive from direct competitive processes. Finally, the third section reports on the numerical simulations, confirms the analytical calculations of the second section, and focuses on the circular-pump case. When the parameter space is inaccessible to theoretical study, numerical investigations are also performed: beyond the numerous behaviors displayed by the system, the effect of the pump polarization on these complex oscillations is emphasized.

I. THE MODEL

The physical arguments for the derivation of the model have been fully developed in the preceding paper [1]. This formulation deals with five ordinary differential equations. The model starts from the Bloch-Maxwell formulation and a double expansion on the transverse angle (θ) and longitudinal coordinate (z) is performed leading to a set of equations governing five variables which are as follows:

(i) Two real population inversions: the usual occupation difference of the lasing levels $D(0,0,\tau)$ averaged on the

fiber length (and also the full zero-order component) and the relative contribution $D(1,0,\tau)$ to the two transverse directions (and the first-order component in θ and the zero-order component in z); and

(ii) Three complex variables: the two transverse polarizations $E_{x,y}(\tau)$ of the total field and the longitudinal grating inside the active medium $D(1,1,\tau)$ corresponding also to the first component in each Fourier series.

The following expansion orders are neglected in a correct way. The Maxwell-Bloch equations give the set

$$(\partial_\tau + 1)E_x(\tau) = d_x \{ E_x(\tau) [D(0,0,\tau) + D(1,0,\tau)] + E_y(\tau) D^*(1,1,\tau) \}, \quad (1.1a)$$

$$(\partial_\tau + K - i\delta)E_y(\tau) = ad_y \{ E_y(\tau) [D(0,0,\tau) - D(1,0,\tau)] + E_x(\tau) D(1,1,\tau) \}, \quad (1.1b)$$

$$\begin{aligned} (\partial_\tau + \gamma)D(0,0,\tau) = & + \gamma P^0 - \gamma \{ \alpha_x |E_x(\tau)|^2 [D(0,0,\tau) + D(1,0,\tau)] + \alpha_y |E_y(\tau)|^2 [D(0,0,\tau) - D(1,0,\tau)] \} \\ & - \frac{\gamma}{2} \{ E_x(\tau) E_y^*(\tau) D(1,1,\tau) d_{xy} + E_y(\tau) E_x^*(\tau) D^*(1,1,\tau) d_{xy}^* \}, \end{aligned} \quad (1.2a)$$

$$(\partial_\tau + \gamma)D(1,0,\tau) = + \gamma P^1 - \gamma \{ \alpha_x |E_x(\tau)|^2 [D(1,0,\tau) + \frac{1}{2}D(0,0,\tau)] + \alpha_y |E_y(\tau)|^2 [D(1,0,\tau) - \frac{1}{2}D(0,0,\tau)] \}, \quad (1.2b)$$

$$(\partial_\tau + \gamma)D(1,1,\tau) = - \gamma D(1,1,\tau) \{ \alpha_x |E_x(\tau)|^2 + \alpha_y |E_y(\tau)|^2 \} - \frac{\gamma}{4} E_y(\tau) E_x^*(\tau) D(0,0,\tau) d_{xy}^*. \quad (1.2c)$$

The parameters $\alpha_{x,y}$ (and $\tilde{\alpha}_{x,y} = \Delta_{x,y} \alpha_{x,y}$) are Lorentzian expressions in terms of the frequency mismatch $\Delta_{x,y}$ between the longitudinal empty cavity modes ($\nu_{x,y}$) and the Bohr frequency (ω) of the active atoms, normalized to the half-width of the homogeneously broadened emission line. They are given by Eqs. (1.13) of Ref. [1]. For an easier understanding of what will follow, we recall that all parameters are normalized to the X -direction losses (κ_x) including the time scale τ, K , the ratio between the two field polarization losses (κ_y/κ_x), γ , the relaxation rate of the population inversions ($2/\kappa_x \tau_3$) related to the lasing level (see Fig. 3 of Ref. [1]), and δ , the direct detuning ($\nu_x - \nu_y/\kappa_x$) between the two empty-cavity frequencies. For notational simplicity, we have also defined $d_{x,y} = \alpha_{x,y} + i\tilde{\alpha}_{x,y}$ and $d_{xy} = (\alpha_x + \alpha_y) + i(\tilde{\alpha}_x - \tilde{\alpha}_y)$.

We note that all the variables and parameters are dimensionless. The normalized complex fields E_x and E_y are expressed in a rotating reference frame at the pulsation ν_x/κ_x following

$$\begin{aligned} \mathcal{E}_x(\tau) &= \sqrt{T_s \mu^2 / 2h^2 \gamma \kappa_x} E_x(\tau), \\ \mathcal{E}_y(\tau) &= \sqrt{T_s \mu^2 / 2h^2 \gamma \kappa_x} E_y(\tau) \\ &\quad \times \exp\left\{ -i \frac{\nu_y}{\kappa_x} \tau \right\} \exp\left\{ i \frac{\nu_x}{\kappa_x} \tau \right\}. \end{aligned} \quad (1.3)$$

The dimensionless population inversion D , defined as $\mathcal{D}(\theta, z, \tau) = [\nu_x T_s \mu^2 / 8h \epsilon_0 \kappa_x]^{-1} D(\theta, z, \tau)$, is expanded in Fourier series at order i (transversely) and j (longitudinally)

which gives us the $D(i,j,\tau)$ variables. The script letters represent the macroscopic variables.

The parameters P^0 and P^1 are, respectively, the pumping rate averaged along the cavity length and the relative contribution to the two directions of the laser emission. (See Appendix A of Ref. [1].)

The steady states of the sets (1.1) and (1.2) can be summarized as follows.

(i) The trivial solution which is the off-operating one where all the variable values are zero except D_{00} which is P^0 and D_{10} which is P^1 .

(ii) The strong mode (SM) solution which corresponds to the X -polarization oscillation in our study since K is taken larger than unity.

(iii) The weak mode (WM) solution or the Y -polarization oscillation (for the case $K > 1$).

(iv) Finally, the bimode solution characterized by the simultaneous oscillation of the two polarizations; this last solution is obtained implicitly but details for small γ are presented in Appendix B of Ref. [1].

Modified variables and parameters being defined for notational convenience as

$$p^0 = \alpha_x P^0, \quad p^1 = \alpha_x P^1, \quad I_x = \alpha_x \mathcal{I}_x, \quad I_y = \alpha_x \mathcal{I}_y, \quad (1.4)$$

$$d_0 = \alpha_x D_{00}, \quad d_{10} = \alpha_x D_{01}, \quad d_{11} = \alpha_x D_{11},$$

the intensities related to the monomode solutions are given by

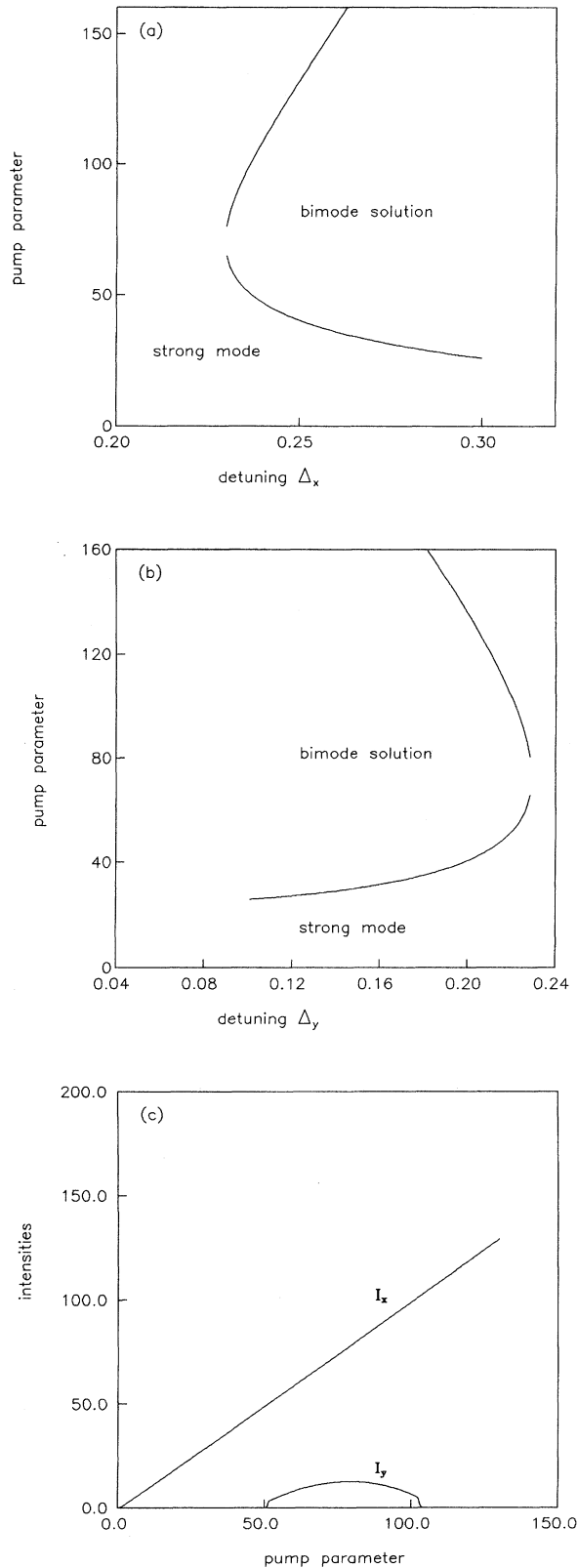


FIG. 1. Bifurcation diagram vs the pump p^0 and (a) Δ_x or (b) Δ_y , for $p^1 = p^0/2$, $a = 1$, $K = 1$, $\gamma = 0.001$, and $\delta = 0.001$, and (c) related stable solutions for $\Delta_x = 0.2$ and $\Delta_y = 0.1$.

$$I_{xs} = \frac{p^0 - 4}{2} + \frac{1}{2}\sqrt{C}, \quad I_{ys} = 0$$

with

$$C = (p^0 - 4)^2 + 8(p^0 + p^1 - 1)$$

and the useful relation

$$d_0 + d_{10} = 1 \quad (1.5)$$

for the strong mode, and

$$I_{xs} = 0, \quad I_{ys} = \frac{1}{2}[(P^0 - 4) + \sqrt{C'}]$$

where

$$C' = (P^0 - 4)^2 + 8(P^0 - P^1 - 1)$$

and

$$d_0 - d_{10} = (K\alpha_x / a\alpha_y) = Q \quad (1.6)$$

for the weak mode.

Before carrying out the linear stability analysis of the monomode steady states, we recall the following exclusive property deduced from the bifurcation theory: the two monomode solutions (SM or WM) never oscillate simultaneously (to produce a bipolarizedlike oscillation). Even if the system is in a multistable situation characterized by the existence and stability of two steady states, when the laser oscillates it chooses one steady state (and only one) depending on the initial conditions (the attraction basin). Thus, when two polarizations are simultaneously present in the laser output, the oscillation is originated necessarily by the bimode solution.

II. LINEAR STABILITY OF MONOMODE STEADY STATES

A. Stability of the "off-operating" laser solution

The general method to analyze the stability of a steady solution \vec{X}_s consists in perturbing the system such that $\vec{X}(\tau) = \vec{X}_s + \varepsilon \vec{X}'(\tau)e^{\lambda\tau}$ where the vector $\vec{X}(\tau)$ stands for the set of five variables $[E_x(\tau), E_y(\tau), D_{00}(\tau), D_{10}(\tau), D_{11}(\tau)]$ and where $\varepsilon \ll 1$. The calculations are performed to the first order in ε . When the system goes back to its steady value ($\text{Re}\lambda < 0$), the stationary state is said to be asymptotically stable. Otherwise ($\text{Re}\lambda > 0$) the state is unstable. The imaginary part of λ is a sign of an oscillatory transient response to the perturbation. The λ are the Lyapunov coefficients for the considered steady branch. In our case, the λ values are given by a characteristic equation of the eighth order (one for each real variable or variety).

Using the previous definitions, the following roots for the characteristic equation are obtained for the trivial solution stability:

$$\lambda_{1,2,3} = -\gamma, \quad (2.1a)$$

$$\lambda_{4,5} = -1 + p^0 + p^1 \pm i\Delta_x(p^0 + p^1), \quad (2.1b)$$

$$\lambda_{6,7} = -K + KQ^{-1}(p^0 - p^1) \pm i\Delta_y(p^0 - p^1) + i\delta \quad (2.1c)$$

$$\lambda_8 = 0. \quad (2.1d)$$

These roots express the existence of a marginal variety (the eighth one), three stable varieties (1, 2, and 3) corresponding to the inversion variables, and four directions that may lead to a destabilization since the real parts of $\lambda_{4,5,6,7}$ cross the imaginary axis and take positive values for, respectively, $p^0 + p^1 > 1$ and $(p^0 - p^1) > Q$. The steady state loses its stability at exactly the threshold of either the strong or the weak modes: then the zero solution becomes unstable above this critical point and the system oscillates following the involved monomode solution. Depending on whether the lower critical point corresponds to the SM or the WM threshold (with respect to a varying parameter), the system displays the associated monomode solution and the higher critical point becomes invalid: the zero solution being unstable in the surroundings of the higher bifurcation point, the validity of the linear stability analysis is not ensured above the first critical point. Moreover, no restabilization of the off-oscillating solution for high pumpings appears since all the roots have positive real parts: the results of this linear stability analysis are definitively valid until the first bifurcation point.

At the critical points, the imaginary parts of the Lyapunov coefficients are, respectively, $\pm i\Delta_x$ and $\pm i(K\Delta_y - \delta)$, which correspond to the frequencies of the X and Y monomode field polarizations. The transient behavior below the first laser threshold is already oscillatory: the zero solution being stable, the perturbed system goes back to its steady state, oscillating around it.

Before analyzing the stability of the monomode state, we point out the following remark.

The bimode solution can never start from the off-lasing state since, first, following the asymptotic approach of Appendix B of Ref. [1], its existence threshold is higher than the monomode oscillation threshold, and, second, we know from the above analysis that the existence domain of the bimode solution does not correspond to the bifurcation (and destabilization) limits of the zero solution since it is higher valued.

At the threshold of the lasing oscillation, the preceding linear stability analysis reports on one monomode steady state. The question is now related to the stability of this lasing state.

B. Strong-mode stability

The stability of the strong branch is governed by an 8×8 matrix which separates into two 4×4 matrices. This represents couplings between the X polarization of the field and the population variables $D(0,0)$ and $D(1,0)$ on the one hand and on the other hand the Y polarization of the field and the complex component of the population inversion representing the grating $D(1,1)$ [3]. This separation confirms the phase instability that may occur via the interferences of the Y

polarization and the grating $D(1,1)$ while the role of $D(1,0)$ is to reinforce the SM steady solution. One obtains two characteristic equations: a real polynomial of the fourth order and a complex polynomial of the second order.

The quartic is

$$\lambda(\lambda^3 + a_2\lambda^2 + a_1\lambda + a_0) = 0, \quad (2.2)$$

where

$$a_2 = [2\gamma(1 + I_{xs})], \quad (2.2a)$$

$$a_1 = \left\{ \gamma^2 \left[(1 + I_{xs})^2 - \frac{I_{xs}^2}{2} \right] + \gamma[I_{xs}(4 - p^0 + I_{xs})] \right\}, \quad (2.2b)$$

$$a_0 = \gamma^2 I_{xs} [4 - p^0 + 2I_{xs}]. \quad (2.2c)$$

All the a_i are positive above the SM threshold and following Abramowitz and Stegun [7] the roots of the cubic always have negative real parts which exclude any instability whose source could be the set of variables $(E_x, D(0,0), D(1,0))$. One can be convinced of the validity of this conclusion using a small- γ expansion of λ (in powers of $\gamma^{1/2}$) since γ is of the order of 10^{-3} [1,6]. The roots are thus given by

$$\lambda_1 = \left(-1 - \frac{[p^0 - 4 + \sqrt{C}]^2}{8(p^0 + p^1 - 1)} \right) \gamma + 0(\gamma^{3/2}), \quad (2.3a)$$

$$\lambda_{2,3} = [\pm i\sqrt{2(p^0 + p^1 - 1)}] \gamma^{1/2} - \frac{3p^0 + 4p^1}{8} \frac{p^0 - 4 + \sqrt{C}}{p^0 + p^1 - 1} \gamma + 0(\gamma^{3/2}), \quad (2.3b)$$

$$\lambda_4 = 0. \quad (2.3c)$$

For pumping values above the SM threshold, the real parts at lowest order are negative and no instability can occur.

The second matrix provides a complex characteristic equation

$$\lambda^2 + a'_1\lambda + a'_0 = 0, \quad (2.4)$$

where

$$a'_1 = \gamma(1 + I_{xs}) + K - i(\delta + \Delta_x) - KQ^{-1}(1 - i\Delta_y)(-1 + 2p^0 - 2I_{xs}), \quad (2.4a)$$

$$a'_0 = \gamma(1 + I_{xs})[K - i(\delta + \Delta_x) - KQ^{-1}(1 - i\Delta_y)] \times (-1 + 2p^0 - 2I_{xs}) + \frac{\gamma}{4} KQ^{-1} I_{xs} (p^0 - I_{xs}) \times [2 + \Delta_x^2 - \Delta_x \Delta_y - i(\Delta_x + \Delta_y)]. \quad (2.4b)$$

A direct study of this second-order equation is not easy to perform. However, and for the small parameter γ , the $\gamma^{1/2}$ expansion leads to the following roots:

$$\lambda_5 = \left[-(1 + I_{xs}) - \frac{1}{4} \frac{I_{xs}(p^0 - I_{xs})[2 + \Delta_x^2 - \Delta_x \Delta_y - i(\Delta_x + \Delta_y)]}{Q + 1 - 2p^0 + 2I_{xs} - i\Delta_y(1 - 2p^0 + 2I_{xs}) - iQK^{-1}(\delta + \Delta_x)} \right] \gamma + 0(\gamma^{3/2}), \quad (2.5a)$$

$$\lambda_6 = \lambda_5,$$

$$\lambda_{7,8} = K[-1 - Q^{-1}(1 - 2p^0 + 2I_{xs}) \pm i[(\delta + \Delta_x) + KQ^{-1}\Delta_y(1 - 2p^0 + 2I_{xs})] + 0(\gamma)]. \quad (2.5b)$$

The real part of the roots ($\lambda_{7,8}$) presents a bifurcation point for $\text{Re}(\lambda_{7,8})=0$. When the condition $p^0 > Q-3$ is realized, the SM is stable for the inequality $Q^2 - 6Q + 1 > 2p^0(Q-3) + 8p^1$. Above this limit, the SM mode becomes unstable: one can note from Eq. (B4b) of Ref. [1] that the existence domain of the Y polarization of the bimode solution starts exactly at this critical point. Moreover, at the bifurcation point, the imaginary part of $\lambda_{7,8}$ is $\delta + \Delta_x - \Delta_y K$ which is just the expression of the D_{11} frequency in the bimode solution. One can then conclude that with this bifurcation point (1) we are dealing with a steady bifurcation which transfers the stability from the SM solution to the bimode oscillation and (2) the ($\lambda_{7,8}$) Lyapunov coefficients are related to the two-dimensional D_{11} variety.

No more evident bifurcation appears from Eqs. (2.5) and the analytic solution of $\text{Re}(\lambda_{5,6})=0$ is not easy to obtain. To get more information on the stability of this mode, asymptotic calculations are needed. They are presented in Appendix A and concern the near-threshold (Appendix A 1) and large-pumpings (Appendix A 2) conditions. We can summarize the results as follows.

No instability is induced by the roots $\lambda_{5,6}$. For realistic values of the parameters, the real part is negative in the two cases (near and far from threshold) and this has been verified by solving the roots of the polynomial (2.4).

If one applies the near-threshold and large-pumping conditions to the two other roots ($\lambda_{7,8}$) the results are the following. Around the SM threshold ($p^0 \approx p_{\text{thr}}^0$), the real part gives at first order the stability condition $Q > 1$ ($Q < \frac{1}{2}$) when the pump polarization is circular (X linear). Then just above threshold the SM is stable only for $Q > Q_i$, Q_i being the intersection point of the curves representing the existence limits of the monomode steady states: the numerical simulations of Figs. 5 and 7 of Ref. [1] showing the parameter conditions for the monomode (SM or WM) oscillation and stabilization are then partially demonstrated.

For a large pump parameter, an asymptotical calculation leads to a restabilized SM but not for all Q values characterizing the SM existence domain. This analytical limitation is due to the simultaneous small-parameter expansions versus γ and the pump parameter.

This restabilization occurs for all Q as can be observed in Figs. 1(a) and 1(b). These graphs display the bifurcation diagram presented by our system versus the pump p^0 and Δ_x or Δ_y while Fig. 1(c) gives the corresponding intensities versus the pumping p^0 . In the case considered, the pumping is X linear. The SM starts oscillating for reasonable pumping values; on increasing the pump rate (and bifurcation parameter) a transfer of stability to the bimode oscillation occurs. This oscillation is stable up to very high values of the pump where the SM appears again. The present work demonstrates this scenario analytically around the following three bifurcation regions: the monomode threshold, the bimode oscillation (but without the corresponding stability), and the monomode high intensities. The parameters for Fig. 1 are $a=1$, $K=1$, $\gamma=0.001$, and $\delta=0.001$, and additionally $\Delta_x=0.2$ and $\Delta_y=0.1$ for Fig. 1(c).

The weak-mode stability will complete the monomode-case analysis.

C. Weak-mode stability

The linear stability study of the weak mode leads qualitatively to the same types of coupling between the variables. This case also produces a separation of the matrix into two parts and two characteristic equations.

The first matrix implicates the oscillating polarization and the real inversions $D(0,0)$ and $D(1,0)$. The resulting polynomial has the form

$$\lambda(\lambda^3 + b_2\lambda^2 + b_1\lambda + b_0) = 0, \quad (2.6)$$

where

$$b_2 = 2\gamma(1 + I_{ys}), \quad (2.6a)$$

$$b_1 = \gamma^2 \left[(1 + I_{ys})^2 - \frac{I_{ys}^2}{2} \right] + \gamma K I_{ys} (4 - Q^{-1}p^0 + I_{ys}), \quad (2.6b)$$

$$b_0 = \gamma^2 K I_{ys} [4 - Q^{-1}p^0 + 2I_{ys}]. \quad (2.6c)$$

All the coefficients are positive which leads to the same conclusions as for the strong mode: when the WM oscillates, $D(0,0)$ and $D(1,0)$ do not originate any instability; these varieties are stable. An expansion versus the small parameter γ leads to the following first-order parameters:

$$\lambda_1 = \left(-1 - \frac{[p^0 - 4B + B\sqrt{C'}]^2}{8B(p^0 - p^1 - B)} \right) \gamma^2 + o(\gamma^{5/2}), \quad (2.7a)$$

$$\lambda_{2,3} = (\pm i \sqrt{2B^{-1}(p^0 - p^1 - B)}) \gamma^{3/2} - \frac{p^0 - 4B + B\sqrt{C'}}{8B(p^0 - p^1 - B)} (3p^0 + 4p^1) \gamma^2 + o(\gamma^{5/2}), \quad (2.7b)$$

$$\lambda_4 = 0. \quad (2.7c)$$

The existence condition for the weak mode implies that all real parts of the above roots are negative. A comparison with the set of equations (2.3) shows, however, that the orders of magnitude of the λ 's are lower, meaning a weaker stability: the system needs a longer time to go back to its stable state.

The coupling of the X mode and the grating $D(1,1)$ gives a characteristic complex second-order equation

$$\lambda^2 + b'_1\lambda + b'_0 = 0, \quad (2.8)$$

where the coefficients are

$$b'_1 = [\gamma(1 + I_{ys}) + 1 - i(K\Delta_y - \delta) - (1 - i\Delta_x)(-Q + 2p^0 - 2QI_{ys})], \quad (2.8a)$$

$$b'_0 = \gamma(1 + I_{ys})[1 - i(K\Delta_y - \delta) - (1 - i\Delta_x)(2p^0 - 2QI_{ys} - Q) + \frac{\gamma}{4} I_{ys}(p^0 - QI_{ys}) \times [2 + \Delta_y^2 - \Delta_x\Delta_y - i(\Delta_x + \Delta_y)]]. \quad (2.8b)$$

The presence of too many parameters makes the analytical solution not useful for a significant analysis. Thus we try a perturbative expansion versus γ which leads to the following roots:

$$\lambda_5 = \left[-(1 - I_{ys}) - \frac{1}{4} \frac{I_{ys}(p^0 - QI_{ys})[2 + \Delta_y^2 - \Delta_x \Delta_y - i(\Delta_x + \Delta_y)]}{1 + Q - 2(p^0 - QI_{ys}) - i\Delta_x[Q - 2(p^0 - QI_{ys})] - i(K\Delta_y - \delta)} \right] \gamma + o(\gamma^{3/2}), \quad (2.9a)$$

$$\lambda_6 = \lambda_5^*,$$

$$\lambda_{7,8} = [-1 - Q + 2(p^0 - QI_{ys})] \pm i[\delta - K\Delta_y + \Delta_x[-Q + 2(p^0 - QI_{ys})]]. \quad (2.9b)$$

A bifurcation point arises with $\text{Re}(\lambda_{7,8})$ and this critical point is characterized by

$$B^2 - 6B + 1 = 2p^0(1 - 3B) - 8Bp^1. \quad (2.10)$$

The WM is stable when both conditions

$$p^0 > 1 - 3B \quad \text{and} \quad B^2 - 6B + 1 < 2p^0(B - 3) + 8p^1$$

are simultaneously realized so that above this limit it becomes unstable. This critical line is identical to the existence limit of the X polarization of the bimode solution. Thus one may suppose that the bimode solution starts at this point, essentially if we notice that, on the bifurcation line, the imaginary part of $\lambda_{7,8}$ is $\delta - K\Delta_y + \Delta_x$.

As for the strong mode, the roots of the equation $\text{Re}(\lambda_{5,6}) = 0$ can be integrated numerically and no instability occurs from these roots in the explored parameter region.

More information on the WM stability may arise from asymptotic calculations. They are presented in Appendix B and lead to the following results. Just above the threshold ($p^0 = p_{\text{thr}}^0 + \varepsilon$, $I_{ys} \approx \varepsilon$), the stability is realized for $Q < 1$ or $\frac{1}{3}$ (depending on the pump polarization) which represents the space below the intersection point Q_i of the monomode-existence domains. Finally, a second bifurcation point is shown to be present for high pumpings leading to a restabilization of the WM oscillation.

The results of the linear stability analysis of the monomode steady states provide a global view based on some symmetry between the WM and SM solutions. Depending on both the pump polarization and detunings, the system starts oscillating in a monomode way. For high pumpings, the destabilizing effect of the grating disappears and the same monomode state oscillates again. We also know from the previous linear stability analysis that a bimode oscillation can take place between these two stable domains of the monomode regime. The resulting questions one may ask concern first the stability of the bipolarized state and the presence and the stability of other types of time-dependent solutions that could be present.

We shall not carry out a linear stability analysis of the bimode solution because of its mathematical complexity. The bimode solution is shown numerically to be always stable in the case of an X -linear pumping. Thus to explore the simultaneous oscillation of the two polarizations one needs to use numerical tools.

III. NUMERICAL SIMULATIONS

A. Parameter choices

The parameter space of our model is multidimensional and thus it cannot be fully treated. A coarse-grained selection

can already be performed following the perturbative analytic calculation which describes typical behaviors in a restricted domain (small γ , for example). In our calculations and from the monomode stability analyses, globally the dynamics induced by the linear or the circular pump polarization are not so different and the space parameter seems to have very little influence on it: one monomode operation always starts stably, then it disappears while the bimode oscillation rises. For this last solution, the numerical simulations of Fig. 1 show a strong stability of the bipolarized solution but only for the X -linear polarization: for a wide range of parameters corresponding to its existence domain, this has been verified numerically.

In the case of a circular pump polarization, the bimode domain of existence is completely unknown. For that reason, we have focused our numerical investigation on this particular pump case.

Because of the large parameter domain, one needs to select physical situations. The parameters a and K are always chosen to be around unity for experimental reasons: the ratio between the optical cavity frequencies is very close to unity as will be seen later and the losses are nearly equal as the cavity quality factor is taken the same for all modes at first approximation. However, the difference between the losses can be increased deliberately.

The three detunings in the problem are Δ_x , Δ_y , and $\delta = (\Delta_x - \Delta_y)\gamma_{\perp}/\kappa_x$ where the ratio γ_{\perp}/κ_x is around 10^{-2} – 10^{-3} for conventional fiber lasers [6]. We have already pointed out the direct correlation between the oscillating monomode and the gap between the mode frequency and the central frequency of the atomic gain curve: the closer the mode is to the center line, which corresponds to the Bohr atomic frequency ω and is about 10^{14} Hz, the more favored is its oscillation. The half-linewidth of this homogeneous gain line is about $2\gamma_{\perp}$ (10^{12} Hz). Thus for cavity frequencies ν_x and ν_y fully antisymmetric with respect to ω , the parameter a reaches its maximum value for $(\omega + \gamma_{\perp})/(\omega - \gamma_{\perp}) = 1.01$ and its minimum for 0.98. As a result unity is already a reasonable value for a .

At half-linewidth of the gain line, the detuning parameters also satisfy the inequality $|\Delta_{x,y}| = \frac{1}{2}$ which requires $0.8 \leq \alpha_{x,y} \leq 1$ and as a result $0.7 \leq Q \leq 1.3$. If one considers Figs. 7(a) and 7(b) of Ref. [1], this limitation leads to two conclusions.

(1) In the case of an X -polarized pump (characterized by an intersection point $Q_i = \frac{1}{3}$), only the SM (X polarization) is presented by the laser and for very high pumpings the bimode (two simultaneous polarizations) oscillates stably.

(2) For a circular pump, all the steady states are accessible for reasonable parameter values ($Q_i \cong 1$).

Thus this “homogeneous-broadening” formulation supposes limited detunings. However, we shall deviate from this description following the next argument: in some experimental setups [6], the laser emission occurs on two field polarizations both of large broadband frequencies which include a high number of modes (nearly 1000). This requires the model to take into account a very large linewidth and an inhomogeneous gain line which is not the case we consider. However, we shall introduce this experimental reality by considering large detuning values, which supposes a very broad gain line, and so that the mode frequencies can be far from the center line (twice or three times γ_{\perp}). This parametric situation has been used to describe semiconductor lasers [4] for which broadness of the emission is observed: this phenomenon is described via the so-called Henry coefficient [5] and is due to the diffusion and mobility of charge carriers inside the conduction band. The Henry coefficient takes high values and is often associated with a detuning parameter [4,8].

Using the same arguments, the a parameter can also take values between 0.7 and 1.3 and in this way some experimental realities are introduced in the model phenomenologically.

One also notes the following experimental feature: for some optical fiber lasers, the parameter δ is of the order of $10(\Delta_x - \Delta_y)$. However, very good cavities are realized using a Bragg grating imprinted in the silica [9]; this leads to very low values of the parameters $\kappa_{x,y}$ so that δ is around $100(\Delta_x - \Delta_y)$. However, this particular parameter domain has not been systematically investigated.

B. Numerical investigation

We first note that all the conclusions resulting from the exact or asymptotical calculations on the stability-domain limits and presented in this paper have been verified by direct integration of the model. In this section we shall present only the investigations related to the circular pump polarization and realized in a parameter space inaccessible to analytical study; it concerns the bimode-regime domain embedded between the lines of destabilization and restabilization of monomode oscillations. This large parametric domain (in P^0 and also in detunings) has been scanned and we present the main characteristic behaviors that have been observed, corresponding or not to experimental situations.

We display in Figs. 2(a) and 2(b) a T -periodic regime (which looks like a Q -switch oscillation) where the extrema of the two polarization intensities are in phase (obtained by superposition of the two figures). This is a signature of the presence of a Hopf bifurcation on the bimode branches which often leads to a Feigenbaum sequence of period doubling for increasing pumping. This dynamical behavior occurs for the following parametric situation: $P^0=6$, $a=0.75$, $K=1.89$, $\gamma=0.004$, $\delta=2.2$, $\Delta_x=3.5$, and $\Delta_y=3.3$. It corresponds to a good laser cavity, high different losses between the two oscillation directions (due to the propagation in the fiber), and especially “inhomogeneous broadening” (and a broad frequency emission). We note that the representation of the Y polarization intensity needs to be multiplied by 10: this is related to the strong losses in the Y direction. This kind of behavior has been observed experimentally [6].

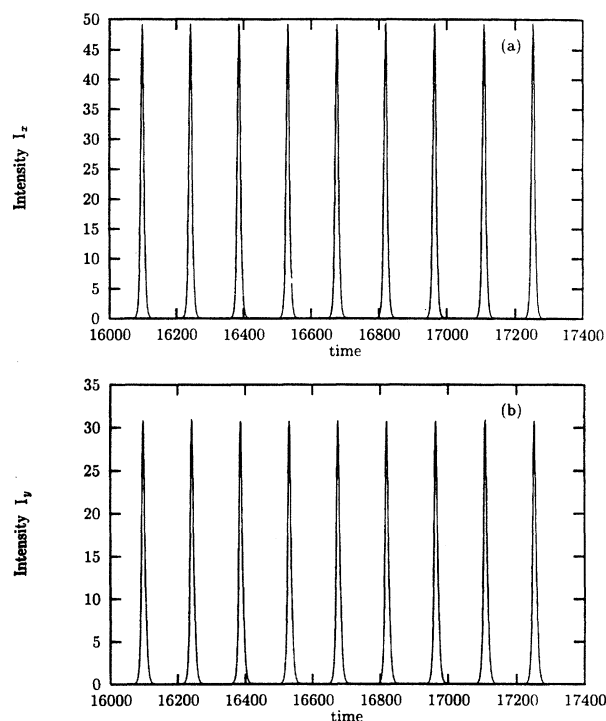


FIG. 2. Intensity T -periodic regime (Q switch) for the parametric situation $P^0=6$, $a=0.75$, $K=1.89$, $\gamma=0.004$, $\delta=2.2$, $\Delta_x=3.5$, and $\Delta_y=3.3$; (a) the X mode; (b) the Y intensity is multiplied by 10.

The second typical time-dependent output that has been measured experimentally and reproduced by our model is a periodic anti-phase regime which indicates the phase sensitivity of the system [8] and describes a mode competition between the two simultaneous modes. The parameters for Fig. 3 are now reasonable (in the “homogeneous broadening and normal cavity losses” meaning): $P^0=4$, $a=1.0$, $K=1.05$, $\gamma=0.001$, $\delta=0.001$, $\Delta_x=0.5$, and $\Delta_y=0.45$. This mode competition is a well-known behavior of conventional multimode lasers.

Chaotic behaviors are also present in several forms. In Figs. 4(a) and 4(b) an intermittency regime for the two polarizations is displayed. Simultaneously an antiphase behavior can be noticed between the two modes: the peaks of one mode increase when those of the second decrease. The parametric situation corresponding to this figure is characterized by an “inhomogeneous broadening” and abnormal cavity losses since $P^0=4$, $a=1.0$, $K=1.8$, $\gamma=0.004$, $\delta=2.1$, $\Delta_x=3.5$, and $\Delta_y=3.3$. The Y intensity is also multiplied by 10.

Two bursting situations (respectively in chaotic and regular regimes) are presented in Figs. 5(a) and 5(b) for, respectively, (a) $P^0=8$, $P^1=3$, $a=1.0$, $K=1.0$, $\gamma=0.004$, $\gamma=0.0$, and $\Delta_x=\Delta_y=0.5$, and (b) $P^0=8$, $P^1=3$, $a=1.0$, $K=1.0$, $\gamma=0.0001$, $\delta=0.0$, $\Delta_x=0.52$, and $\Delta_y=0.5$. The main characteristic of this parameter space is that either the spontaneous emission is not negligible and is polarization dependent, or the dipole transverse distribution leads to this special pump sharing: an idea of the difficulty in managing such a parameter space is given. One can note, however, that

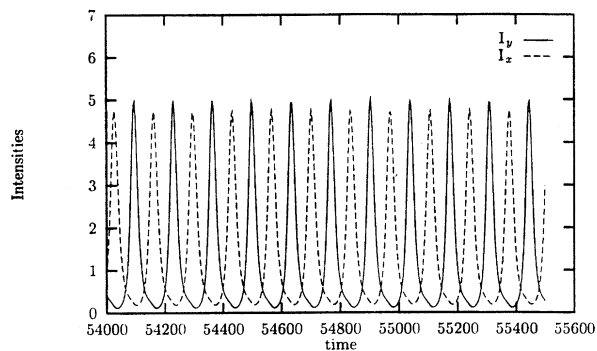


FIG. 3. Intensity T -periodic antiphase regime describing competition between the two modes. The parameters are $\mathcal{P}^0=4$, $a=1.0$, $K=1.05$, $\gamma=0.001$, $\delta=0.001$, $\Delta_x=0.5$, and $\Delta_y=0.45$.

equal detunings lead to a real bursting situation (meaning a chaotic hesitation around a solution) with high peaks in intensity while a slight difference (in favor of the Y direction) between the detunings produces a regular bursting: a nearly Q switch for the Y mode and hesitation for the X mode. An elliptic pump can also provide such outputs.

Finally Figs. 6(a) and 6(b) give the bifurcation diagram versus \mathcal{P}^0 of, respectively, the X and Y polarizations for a circular pump. This corresponds to a detailed transverse section of a graph similar to the one represented in Fig. 1. It shows a chaotic behavior embedded in the bimode stable domain. The parameters are $a=1.0$, $K=1.01$, $\gamma=0.03$,

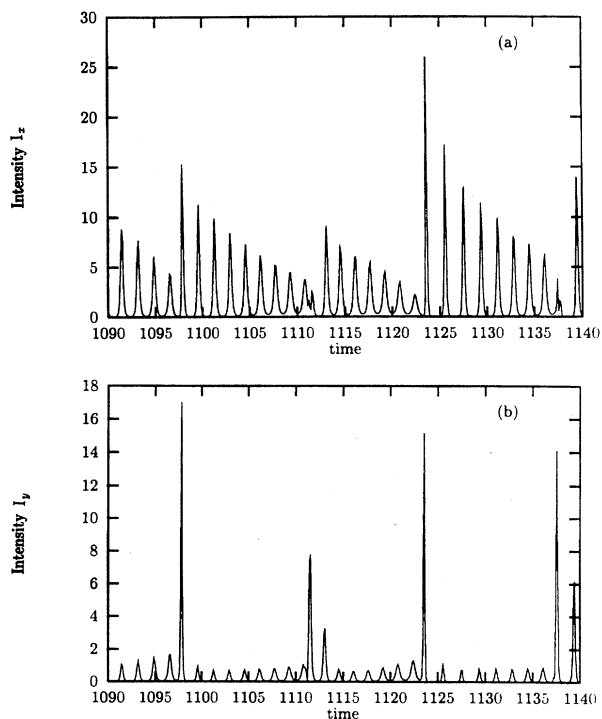


FIG. 4. Antiphase chaotic situation in intensity for $\mathcal{P}^0=4$, $a=1.0$, $K=1.8$, $\gamma=0.004$, $\delta=2.1$, $\Delta_x=3.5$, and $\Delta_y=3.3$. In (b) the Y intensity is multiplied by 10.

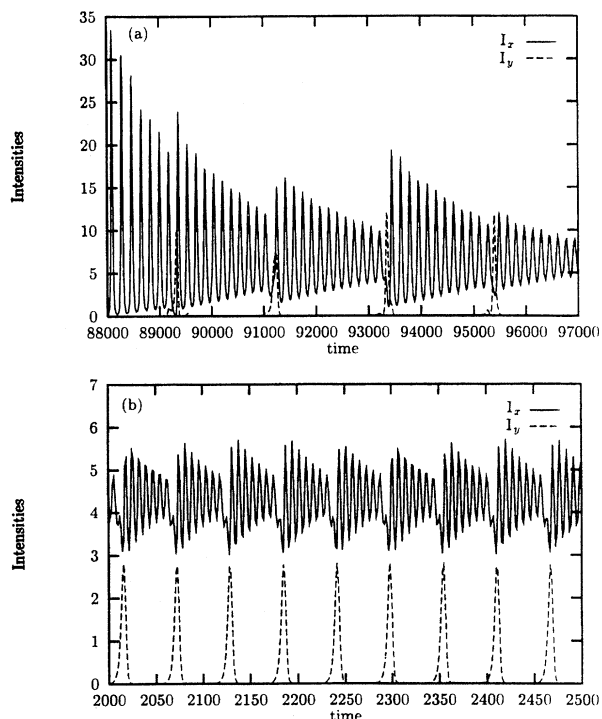


FIG. 5. Chaotic and regular bursting situations for (a) $\mathcal{P}^0=8$, $\mathcal{P}^1=3$, $a=1.0$, $K=1.0$, $\gamma=0.004$, $\delta=0.0$, and $\Delta_x=\Delta_y=0.5$ and (b) $\mathcal{P}^0=8$, $\mathcal{P}^1=3$, $a=1.0$, $K=1.0$, $\gamma=0.0001$, $\delta=0.0$, $\Delta_x=0.52$, and $\Delta_y=0.5$.

$\delta=0.0$, and $\Delta_x=\Delta_y=0.8$. A characterization of this chaotic behavior is now in progress.

IV. CONCLUSION

In this study, we have derived and carefully analyzed a vectorial model for a doped fiber laser whose two transverse field polarizations are allowed to oscillate. The parameter space of the problem has been investigated focusing essentially on the polarization of the pump and the detuning effects. The analytical calculations have been carried out as far as possible including asymptotic expansions whose validity extends beyond the expected parametric space, as shown numerically.

In summary, we have found that the linear pump polarization allows first the oscillation of its own type of polarization [10] but for higher pump intensities and because of the polarized medium the two directions oscillate stably [6,9]. It can also present an oscillation on the complementary transverse direction when the losses or the detunings are strongly favorable.

The circular pump polarization presents a wealth of dynamical behaviors as each polarized oscillation may easily be present: this depends mainly on the detunings of the two modes. Increasing the pumping, two polarizations (bipolarized state) arise simultaneously and are stable; they can oscillate in phase or in antiphase presenting mode competition. Periodic and chaotic regions are also displayed, which are characterized by antiphase and bursting. Thus we conclude the following.

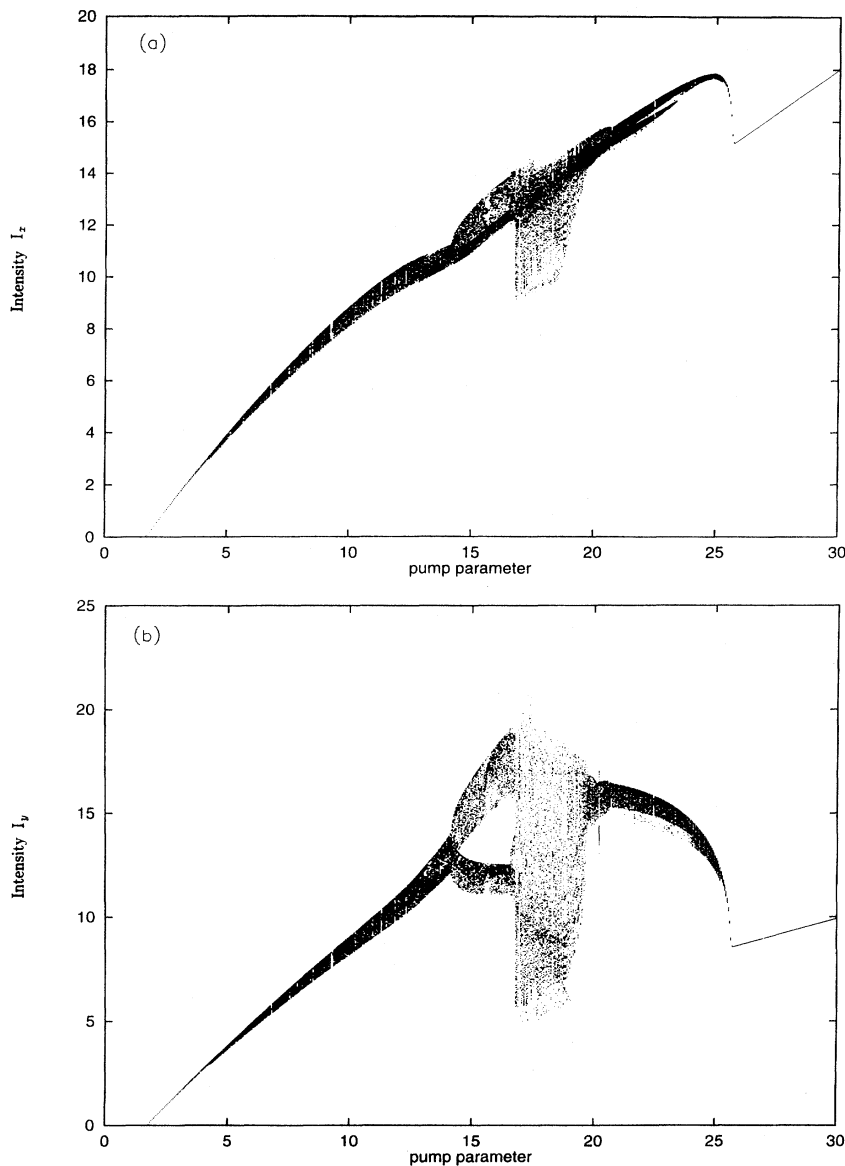


FIG. 6. Chaotic bifurcation diagram vs the pump \mathcal{P}^0 in the bimode domain for (a) the X mode and (b) the Y mode. The parameters are $a=1.0$, $K=1.01$, $\gamma=0.03$, $\delta=0.0$, and $\Delta_x=\Delta_y=0.8$.

(1) The transverse-oriented pump favors the stable oscillation of one direction but it does not exclude the other transverse oscillation alone (under drastic conditions) or in a bimode stable output. However, it destroys all the instabilities since only steady states are present.

(2) In contrast, the circular pump does not act like a “forcing.” Therefore the nonlinearities due to the interaction between the light and polarized medium express their dynamics fully and combine in diverse ways the effects of detunings and medium activity.

One can infer the strong role of the pump since many time-dependent behaviors can be extinguished in favor of the preferentially oriented oscillation and very large pumpings and detunings can be necessary for the oscillation of the complementary direction.

The second element to point out is that, whatever the pump, the presence of the “transverse” population inversion D_{10} clearly stabilizes the monomode and also the bimode oscillations: this last operation was impossible to realize in

the counterpropagative ring laser and the bimode semiconductor laser.

In the experiments, bipolarized laser operation occurs on a broad mode band and has a large-linewidth emission. As a result, the homogeneous Lorentzian atomic profile is certainly not adapted to this problem. This supposes an inhomogeneous contribution whose origin will be related to the active atoms (and their sites) or to the host medium (silica) where the propagation occurs. A formulation of basic equations containing an inhomogeneous (anisotropic) transverse distribution of the dopant is also possible but it is not enough for a full description of the OFL. Many other anisotropic effects have to be included in the description. In spite of the numerous simplifications which were introduced, the model presents some agreement with the dynamics experimentally observed. It is, however, very much a first and imperfect approach to the description of an optical fiber laser since no propagating effects are included. This last phenomenon includes necessarily the multimode nature of the laser field and

is now being studied on its own before an extension to a model which mixes light nonlinearities in matter (caused by vectorial interactions) and propagation.

ACKNOWLEDGMENTS

The authors wish to thank Professor P. Glorieux, Dr. D. Derozier, and Dr. S. Bielawsky for fruitful discussions and their encouragement. The Laboratoire de Spectroscopie Hertzienne is both a university laboratory and associated with the CNRS (URA 249).

APPENDIX A

1. Near-threshold stability of the strong mode

The SM is characterized in the near-threshold situation by the following relations.

(a) For a circular pump polarization $p^1=0$ and $p^0=1+\eta$ ($\eta \ll 1$). The steady intensity takes the value $I_{xs}=2\eta/3$, and the Lyapunov coefficients have the form

$$\text{Re}(\lambda_{5,6}) = -1 - \frac{\eta}{6} \frac{4Q^2 + 4\Delta^2 + Q(\Delta_x^2 - \Delta_x\Delta_y - 6) + \Delta(\Delta_x - 7\Delta_y) + 3(1 + \Delta_y^2) - (1 + \Delta_x^2)}{(Q-1)^2 + (\Delta_y - \Delta)^2}, \quad (\text{A1a})$$

$$\lambda_{7,8} = -\frac{K}{Q} \left[Q - 1 - \frac{2\eta}{3} \pm i \left(\Delta - \Delta_y - \frac{2\eta}{3} \Delta_y \right) \right]. \quad (\text{A1b})$$

We have defined Δ as $(Q/K)(\delta + \Delta_x)$. At the lowest order in η , the real part of $\lambda_{5,6}$ is always negative while the real part of $\lambda_{7,8}$ is negative only for $Q > 1$. Therefore the SM starts oscillating stably above the intersection point of the steady representative curves (see Fig. 7(a) of Ref. [1]; the question mark related to SM stability needs to be canceled).

(b) In the case of a linear pump polarization and near the SM threshold the pump rates are $p^1=p^0/2$ and $p^0=\frac{2}{3}+\eta$ ($\eta \ll 1$). The steady intensity is then $I_{xs}=9\eta/10$ and the Lyapunov coefficients take the form

$$\text{Re}(\lambda_{5,6}) = -1 - \frac{9\eta}{20} \frac{18(Q^2 + \Delta^2) - 3Q(\Delta_x^2 - \Delta_x\Delta_y + 6) - 3\Delta(\Delta_x + 3\Delta_y) + 3(1 + \Delta_y^2) + (1 + \Delta_x^2)}{(3Q-1)^2 + (\Delta_y - 3\Delta)^2}, \quad (\text{A2a})$$

$$\lambda_{7,8} = -\frac{K}{Q} \left[Q - \frac{1}{3} - \frac{\eta}{10} \pm i \left(\Delta - \frac{1}{3}\Delta_y - \frac{\eta}{10}\Delta_y \right) \right]. \quad (\text{A2b})$$

At the lower order, the real part of $\lambda_{5,6}$ is always negative while the $\lambda_{7,8}$ real part is negative only for $Q > \frac{1}{3}$. Hence the strong mode also oscillates stably only above the intersection point of the steady state curves. On Fig. 7(b) of Ref. [1], the SM question mark must also be suppressed.

2. Strong-mode stability for large pumping

For large pumpings (even unrealistic values from the experimental point of view), the steady state is given by the following relations.

(a) For a circular pump polarization $p^1=0$ and $1/p^0=\eta$ ($\eta \ll 1$). The steady intensity takes the value $I_{xs}=p^0-2+2\eta$ and the Lyapunov coefficients have the form

$$\text{Re}(\lambda_{5,6}) = -\frac{p^0 2(Q^2 + \Delta^2) + Q(\Delta_x^2 - \Delta_x\Delta_y - 10) + \Delta(\Delta_x - 11\Delta_y) + 15(1 + \Delta_y^2) - 3(1 + \Delta_x^2)}{(Q-3)^2 + (3\Delta_y - \Delta)^2} \quad (\text{A3a})$$

$$\lambda_{7,8} = -\frac{K}{Q} [Q - 3 + 4\eta \pm i(\Delta - 3\Delta_y + 4\eta\Delta_y)]. \quad (\text{A3b})$$

The relevant term of the $\lambda_{5,6}$ real part is always negative for the usual laser parameters. As a result no instability can occur via these varieties. This has been verified by numerical simulations.

The $\lambda_{7,8}$ are negative again for $Q > 3$. Therefore this mode restabilizes for high values of the pump parameter. This does not mean that for $1 < Q < 3$ there is no restabilization: the calculation being performed for small γ and large p^0 , the product γp^0 can be around unity. Thus one has to be careful: in our case the restabilization line is lost for $1 < Q < 3$ because one needs much larger p^0 values and at least the next order in γ .

To be convinced of the validity of these arguments, we have treated the large- p^0 case without restricting γ to small values. The real parts of the roots of the characteristic equation have been found to be equal to, respectively, $-\gamma p^0$ and $-(K/2Q)[2Q - 4 + \Delta_x^2 - \Delta_x\Delta_y]$. This last expression represents a restabilization of the strong mode for $Q > [4 - \Delta_x(\Delta_x - \Delta_y)]/2$; this Q limit is around 2.

(b) For an X-linear pump ($p^1=p^0/2$), the steady intensity is given by $I_{xs}=p^0-1+\eta$ and the Lyapunov coefficients take the form

$$\text{Re}(\lambda_{5,6}) = -\frac{p^0}{4} \frac{4(Q^2 + \Delta^2) - Q(\Delta_x^2 - \Delta_x \Delta_y + 10) - \Delta(\Delta_x + 9\Delta_y) + 5(1 + \Delta_y^2) + (1 + \Delta_x^2)}{(Q-1)^2 + (\Delta_y - \Delta)^2}, \quad (\text{A4a})$$

$$\lambda_{7,8} = -\frac{K}{Q} [Q - 1 - 2\eta \pm i(\Delta - \Delta_y + 2\eta\Delta_y)]. \quad (\text{A4b})$$

The conclusions are the same as for circular-polarization pumping: a negative $\lambda_{5,6}$ real part and a restabilization of the SM for large values of the pump when $Q > 1$ but this time the restabilization is lost between $\frac{1}{3}$ and unity.

As for the near-threshold case, we have evaluated the Lyapunov roots for a large pumping relaxing the small- γ condition. The real parts of the characteristic equation roots have been found to be equal, respectively, to $-\gamma p^0$ and $-(K/4Q)[4Q - 2 + \Delta_x^2 - \Delta_x \Delta_y]$. This last expression presents a restabilization of the strong mode for $Q > [2 - \Delta_x(\Delta_x - \Delta_y)]/4$ whose value is close to $\frac{1}{3}$.

APPENDIX B

1. Near-threshold stability of the weak mode

The weak mode (Y polarization) is characterized in the near threshold situation by the following relations.

(a) For a circular pump polarization p^0 is written as $Q + \eta$ ($\eta \ll 1$) and the steady intensity takes the value $I_{ys} = 2\eta/3Q$. The Liapunov coefficients have the form

$$\text{Re}(\lambda_{5,6}) = -1 - \frac{\eta}{6Q} \frac{4 + 4\Delta'^2 + Q(\Delta_y^2 - \Delta_x \Delta_y - 6) - Q\Delta'(\Delta_y - 7\Delta_x) + Q^2(2 - \Delta_y^2 + 3\Delta_x^2)}{(Q-1)^2 + (Q\Delta_x - \Delta')^2}, \quad (\text{B1a})$$

$$\lambda_{7,8} = -\left[1 - Q - \frac{2\eta}{3}\right] \pm i\left[\Delta' + \Delta_x\left(Q + \frac{2\eta}{3}\right)\right], \quad (\text{B1b})$$

where we have imposed $\Delta' = \delta - K\Delta_y$. These two roots show that the WM is stable in the surroundings of its threshold for $Q < 1$ and as a result below the intersection point Q_i .

(b) For a linear pump polarization the pump parameter and the steady intensity are, respectively, $p^0 = 2Q + \eta$ ($\eta \ll 1$) and $I_{ys} = \eta/2Q$. The roots of the characteristic equation are now

$$\text{Re}(\lambda_{5,6}) = -1 - \frac{\eta}{4Q} \frac{2 + 2\Delta'^2 + Q(\Delta_y^2 - \Delta_x \Delta_y - 10) - Q\Delta'(\Delta_y - 11\Delta_x) + 3Q^2(4 - \Delta_y^2 + 5\Delta_x^2)}{(3Q-1)^2 + (3Q\Delta_x - \Delta')^2}, \quad (\text{B2a})$$

$$\lambda_{7,8} = -[1 - 3Q - \eta] \pm i[\Delta' + \Delta_x(3Q + \eta)]. \quad (\text{B2b})$$

The relevant orders of the roots $\lambda_{5,6}$ present negative real parts while the roots $\lambda_{7,8}$ show a stable behavior of the WM just above its threshold but only for $Q < \frac{1}{3}$: this allows the general conclusion concerning the stable Y -polarization oscillation just above the lasing point and only below the intersection point of the steady curves representing the threshold intensities versus the Q parameter.

2. Weak-mode stability in the case of high pumping

In the case of large pumpings, the steady state is obtained as follows.

(a) For a circular pump polarization and if we note $1/p^0 = \eta$ ($\eta \ll 1$), the intensity can be written as $I_{ys} = p^0/Q - 2 + 2Q\eta$ and the Lyapunov coefficients have the form

$$\text{Re}(\lambda_{5,6}) = -p^0 \frac{2(1 + \Delta'^2) + Q(\Delta_y^2 - \Delta_x \Delta_y - 10) - Q\Delta'(\Delta_y - 11\Delta_x) + 3Q^2(4 + 5\Delta_x^2 - \Delta_y^2)}{2Q[(3Q-1)^2 + (3Q\Delta_x - \Delta')^2]}, \quad (\text{B3a})$$

$$\lambda_{7,8} = -[1 - 3Q + 4Q^2\eta] \pm i[\Delta' + Q\Delta_x(3 - 4Q\eta)]. \quad (\text{B3b})$$

At the lower order, the real part of $\lambda_{5,6}$ is always negative while that of $\lambda_{7,8}$ is negative only for $Q < \frac{1}{3}$. As a result the weak mode restarts oscillating stably for high pumping only for the previous condition. In the range $\frac{1}{3} < Q < 1$, we use an alternative method: the large- p^0 case without restriction on γ is treated. The real part of the roots have been found

to be proportional to $-\gamma p^0/Q$ and $-[1 - 2Q + Q\Delta_y(\Delta_y - \Delta_x)/2]$. This last expression may present a restabilization of the weak mode for $Q < 2/[4 - \Delta_y(\Delta_y - \Delta_x)]$ whose value is around $\frac{1}{2}$. This increases the restabilization parametric domain.

(b) When $p^1 = p^0/2$ and with the same small parameter

η , the steady intensity is $I_{ys} = p^0/Q - 3 + Q\eta$ and the Liapunov coefficients have the form

$$\text{Re}(\lambda_{5,6}) = -\frac{p^0 u_2}{4Q[(5Q-1)^2 + (5Q\Delta_x - \Delta')^2]}, \quad (\text{B4a})$$

$$\lambda_{7,8} = -[1 - 5Q + 2Q^2\eta] \pm i[\Delta' + Q\Delta_x(5 - 2Q\eta)], \quad (\text{B4b})$$

where u_2 is

$$u_2 = 4(1 + \Delta'^2) + Q(3\Delta_y^2 - 3\Delta_x\Delta_y - 34) - Q\Delta'(3\Delta_y - 37\Delta_x) + 5Q^2(14 - 3\Delta_y^2 + 17\Delta_x^2).$$

The roots $\lambda_{5,6}$ always present negative real parts for realistic parameter values, while $\text{Re}(\lambda_{7,8})$ is negative only for $Q < \frac{1}{5}$. With this calculation, the WM restabilization is demonstrated to occur only for low Q .

Relaxing the small- γ condition, the large-pumping situation leads to real parts of the characteristic equation roots equal, respectively, to $-\gamma p^0/Q$ and $-[1 - 7Q/2 + 3Q\Delta_y(\Delta_y - \Delta_x)/4]$. This last expression may present a restabilization of the weak mode for $Q < 4/[14 - 3\Delta_y(\Delta_y - \Delta_x)]$ and this value is about $\frac{2}{7}$, approaching $\frac{1}{3}$.

-
- [1] H. Zeghlache and A. Boulnois, *Phys. Rev. A* **52**, 4229 (1995).
 [2] K. C. Reiser and L. W. Casperson, *J. Appl. Phys.* **51**, 6075 (1980); **51**, 6083 (1980); S. H. Jiang and L. W. Casperson, *ibid.* **69**, 1866 (1991); L. W. Casperson, *ibid.* **69**, 8005 (1991); L. W. Casperson, W. J. Sandle, A. C. Wilson, D. M. Warrington, and R. J. Ballagh, *ibid.* **69**, 8005 (1991).
 [3] Paul Mandel and G. P. Agrawal, *Opt. Commun.* **42**, 269 (1982); Paul Mandel and N. B. Abraham, *ibid.* **51**, 87 (1984); H. Zeghlache, Paul Mandel, N. B. Abraham, L. M. Hoffer, G. L. Lippi, and T. Mello, *Phys. Rev. A* **37**, 3704 (1988).
 [4] C. Etrich, Paul Mandel, N. B. Abraham, and H. Zeghlache, *IEEE J. Quantum Electron.* **QE-28**, 811 (1992).
 [5] C. H. Henry, *IEEE J. Quantum Electron.* **QE-18**, 259 (1982).
 [6] S. Bielawski, D. Derozier, and P. Glorieux, *Phys. Rev. A* **46**, 2811 (1992); *Opt. Commun.* **83**, 97 (1991).
 [7] *Handbook of Mathematical Functions*, edited by M. Abramowitz and I. Stegun (Dover, New York, 1972), p. 17.
 [8] Paul Mandel, C. Etrich, and Kenju Otsuka, *IEEE J. Quantum Electron.* **QE-29**, 836 (1993).
 [9] E. Delvaque, Ph.D. thesis, Centre National d'Etudes en Telecommunications Lannion and University of Lille, 1993; R. Leners, P. L. Francois, and G. Stéphan, *Opt. Lett.* **19**, 275 (1994); R. Leners, Ph.D. thesis, CNET Lannion, 1994; E. Lacot, F. Stoeckel, and M. Chenevier, *Phys. Rev. A* **49**, 3997 (1994); E. Lacot, Ph.D. thesis, Université J. Fourier, Grenoble, France, 1992.
 [10] J. T. Lin, P. R. Morkel, L. Reekie, and D. N. Payne, in *Proceedings of ECOC'87, Helsinki, Finland, 1987* (ECOC, Helsinki, 1987), Vol. I, pp. 109–112; J. T. Lin, W. A. Gambling, and D. N. Payne, in *Proceedings of CLEO '89, Baltimore, 1989* (CLEO, Baltimore, 1989), Vol. I, pp. 90–91; J. T. Lin and W. A. Gambling, *Proceedings of IEEE Colloquium '90, London, 1989*, (IEEE, London, 1989), p. 10.